

*Effect of complex magnetic structure on
the magnetocaloric and magneto-transport
properties in GdCuSi*

**Sachin Gupta, K. G. Suresh &
A. V. Lukoyanov**

Journal of Materials Science

Full Set - Includes 'Journal of Materials
Science Letters'

ISSN 0022-2461

J Mater Sci

DOI 10.1007/s10853-015-9116-8



 Springer

Your article is protected by copyright and all rights are held exclusively by Springer Science +Business Media New York. This e-offprint is for personal use only and shall not be self-archived in electronic repositories. If you wish to self-archive your article, please use the accepted manuscript version for posting on your own website. You may further deposit the accepted manuscript version in any repository, provided it is only made publicly available 12 months after official publication or later and provided acknowledgement is given to the original source of publication and a link is inserted to the published article on Springer's website. The link must be accompanied by the following text: "The final publication is available at link.springer.com".

Effect of complex magnetic structure on the magnetocaloric and magneto-transport properties in GdCuSi

Sachin Gupta¹  · K. G. Suresh¹ · A. V. Lukoyanov^{2,3}

Received: 11 March 2015 / Accepted: 18 May 2015
© Springer Science+Business Media New York 2015

Abstract GdCuSi has been studied by structural, magnetic, magneto-thermal, and magneto-transport measurements. The compound crystallizes in the Ni₂In-type hexagonal structure. Magnetic measurements show antiferromagnetic ordering at $T_N = 14.2$ K and a magnetic anomaly near 5 K, which are confirmed by different measurements. Magnetocaloric effect (MCE) has been estimated from both magnetization and heat capacity data and it shows a change in sign below T_N . Similar to MCE, magnetoresistance (MR) data also show sign change below T_N . The compound shows large MCE and MR near its ordering temperature. The sign change in MCE and MR is attributed to the non-collinear antiferromagnetic structure of the compound. The theoretical calculations suggest competition of ferromagnetic and antiferromagnetic interactions, which causes non-collinear magnetic structure in this compound.

Introduction

RTX (R = rare earth, T = transition metal, and X = IIIA/IVA block element) family is found to show many intriguing physical properties depending mainly on their crystal structures. A recent review by some of us has

thrown light into these properties [1]. The crystal structure of this family changes upon varying T and X elements. The RCuSi series, which is constituent of the RTX family, is found to show some interesting physical properties. Previous reports show that RCuSi compounds have two types of hexagonal crystal structures; the high temperature phase is AlB₂ associated with the space group P6/mmm and the low temperature phase is found to be in the Ni₂In with space group, P6₃/mmc [2]. Depending on the crystal structure, the compounds show different magnetic properties [2–4]. It has been observed that RCuSi (R = Pr, Gd, Tb) compounds with AlB₂ type structure show ferromagnetic ordering with $T_C = 14$ K for PrCuSi, 49 K for GdCuSi, and 47 K for TbCuSi [2, 3], while RCuSi (R = Gd, Tb) compounds with Ni₂In-type structure show antiferromagnetic ordering with $T_N = 14$ K for GdCuSi and 16 K for TbCuSi [2, 4]. CeCuSi shows ferromagnetic nature below 15.5 K [5]. DyCuSi and HoCuSi show sine wave modulated structures; however, the magnetic ordering in these compounds is stable from 1.4 K to their T_N [6]. These two compounds, DyCuSi [7] and HoCuSi [8], which show antiferromagnetic ordering at 10 and 7 K, respectively, exhibit very large magnetic entropy change near their ordering temperatures. NdCuSi, which is antiferromagnetic at low temperatures also shows very interesting magnetic and transport properties [9]. Papamantellos et al. reported that ErCuSi shows antiferromagnetic ordering below $T_N = 6.8$ K with a transversal amplitude-modulated structure, which transforms to a square up transition to an antiphase domain structure below 3.5 K [10]. TmCuSi is reported to show a complex magnetic structure. Below 5.1 K, it is ferromagnetic and its magnetic structure changes to antiferromagnetic above 5.1 K and the antiferromagnetic order is retained up to $T_N = 6.1$ K [10, 11]. Magnetic properties and ¹⁵⁵Gd hyperfine interaction

✉ Sachin Gupta
gsachin55@gmail.com

¹ Department of Physics, Indian Institute of Technology Bombay, Mumbai 400076, India

² Institute of Metal Physics, Russian Academy of Sciences, Ural Branch, Yekaterinburg 620137, Russia

³ Ural Federal University, Yekaterinburg 620002, Russia

parameters for ternary intermetallic GdTX alloys have recently been discussed by Pöttgen et al. [12].

In this paper, we study the structural, magnetic, thermal, magnetocaloric, and magneto-transport properties of GdCuSi compound along with electronic structure calculations. This compound was studied earlier by some researchers [3, 4, 13], who reported basic structural and magnetic properties. According to these reports, AlB₂ phase of GdCuSi has ferromagnetic ordering at 49 K, while Ni₂In phase shows antiferromagnetic ordering near 14 K [3, 4]. The method of preparation is seen to play a crucial role in determining the phase.

Experimental and computational details

The preparation of polycrystalline GdCuSi was done by arc melting of the constituent elements (Gd with purity 99.9 % and Cu, Si with purity 99.99 %) taken in stoichiometric proportion in a water-cooled copper hearth under argon atmosphere. The alloy ingot was melted several times for a good homogeneity. Subsequently, it was sealed in an evacuated quartz tube and annealed for a period of 10 days at 850 °C followed by furnace cooling. The magnetic $M(T,H)$ and heat capacity $C(T)$ measurements were carried out in a Quantum Design, Physical Property Measurement System (PPMS-6500). The heat capacity measurements were performed using the thermal relaxation technique. The resistivity (ρ) measurements were done in a home-made set up using standard four probe technique with an excitation current of 100 mA.

Ab initio calculations of the electronic structure and magnetic properties were performed with the LDA+U+SO method [14], combining local density approximation LDA and corrections for strong electronic correlations and spin-orbit coupling of the Gd 4f electrons. The following orbital basis set was used: Gd (6s, 6p, 5d, 4f), Cu (4s, 4p, 3d), and Si (3s, 3p, 3d) states, with muffin-tin orbitals radii: $R_{\text{Gd}} = 3.8$ a.u. and $R_{\text{Cu,Si}} = 2.6$ a.u. The values of the direct Coulomb $U = 6.7$ eV and exchange Hund $J_{\text{H}} = 0.7$ eV parameters for the Gd 4f shell were used. The calculations were performed using the experimental values of the lattice parameters.

Experimental results

The phase purity of the annealed sample was examined by the Rietveld analysis at room temperature using powder X-ray diffraction (XRD) pattern, collected on an X'Pert Pro diffractometer using Cu K α ($\lambda = 1.54$ Å) radiation. The refinement shows no detectable impurity and hence

confirms the single phase nature of the compounds. We find that GdCuSi crystallizes in Ni₂In-type hexagonal structure with the space group P6₃/mmc (SG#194). The lattice parameters obtained from the least square fit are found to be $a = b = 4.1679(9)$ Å, $c = 7.5760(2)$ Å and are very close to those reported in literature [4, 13]. The XRD pattern with Rietveld refinement is shown in Fig. 1.

In this section, we discuss the detailed magnetic properties of GdCuSi. The temperature dependence of dc magnetic susceptibility (DCS) along with the inverse magnetic susceptibility is shown in Fig. 2, which shows a cusp-like nature at $T_{\text{N}} = 14.2$ K, suggesting antiferromagnetic ordering at lower temperatures. Below T_{N} , there is a kink near 5 K, denoted as T_{t} , which may be attributed to a spin reorientation transition. The T_{N} estimated from our data matches with that reported in Ref. [4]. However, there is no mention about the other anomaly (at ~ 5 K), though it can be seen in their plot [4]. Fig. 2 also shows the inverse susceptibility data fitted to the Curie–Weiss law, $\chi^{-1} = (T - \theta_{\text{p}})/C_{\text{m}}$, where C_{m} is molar Curie constant in the paramagnetic regime. The values of effective magnetic moment (μ_{eff}) and the paramagnetic Curie temperature (θ_{p}) estimated from the fit are 8.1 μ_{B} and 11.7 K, respectively. The value of calculated μ_{eff} is slightly higher than the free rare earth ion magnetic moments and is close to the reported value [4]. It is worth to note that the existence of an excess magnetic effective or saturation moment is very characteristic phenomenon for Gd ternary intermetallic alloys as mainly caused by the strong polarization of 5d conduction electrons via 4f–5d interaction and this phenomenon is especially well seen for GdAuMg [15], GdAuCd [16], or GdPdCd [17] alloys.

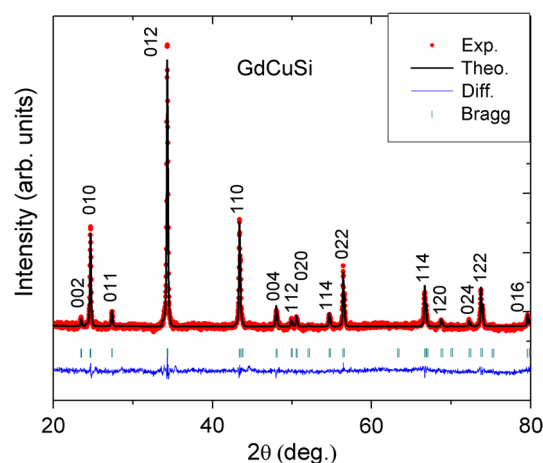


Fig. 1 Powder X-ray diffraction pattern at room temperature along with the Rietveld refinement for GdCuSi. The lower plot shows difference between the experimentally observed and the theoretically calculated patterns

The positive sign of θ_p is an indication of non-collinear magnetic structure at low temperatures. It is also worth noting that the θ_p value is lower than T_N , which may be attributed to the presence of some ferromagnetic correlations [14, 18]. To know about the exact magnetic transition temperature, we have also performed ac susceptibility (ACS) measurements at different frequencies ($f = 25\text{--}625$ Hz) and in constant ac field ($H_{ac} = 1$ Oe), as shown in Fig. 3. It can be seen that the real part (χ') of ACS shows a peak near T_N and an anomaly at about 5 K, consistent with the DCS data.

Figure 4 depicts the magnetization isotherms for fields up to 50 kOe for GdCuSi. Initially, the magnetization increases with increase in temperature (below T_N), but the trend reverses beyond 20 kOe. The inset in Fig. 4 shows the derivative of magnetization with respect to field. One can see from this plot that the peak gets suppressed and shifts to lower field on increasing the temperature. The peak in dM/dH versus H plots indicates the occurrence of a metamagnetic transition. The value of critical field is

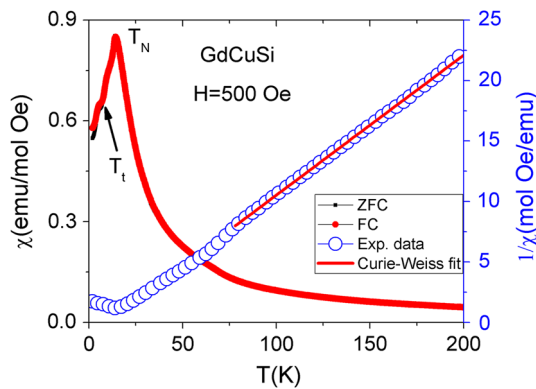


Fig. 2 Temperature dependence of magnetic susceptibility along with Curie-Weiss fit for GdCuSi

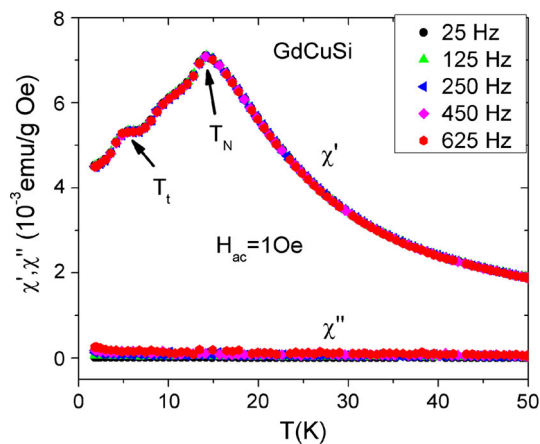


Fig. 3 Temperature dependence of ac susceptibility for GdCuSi at different frequencies ($f = 25\text{--}625$ Hz) and in constant ac field ($H_{ac} = 1$ Oe)

calculated to be 20.8 kOe at 4 K. The compound shows negligible magnetic hysteresis and no sign of magnetic saturation for fields up to 50 kOe. Rapid change in magnetization isotherms near the magnetic ordering temperatures gives an indication about large magnetic entropy change in this compound.

To explore the magnetic state further, the heat capacity measurements were carried out in 0 and 50 kOe fields in the temperature range of 2–100 K and the data are plotted in Fig. 5. The heat capacity data show a peak near the magnetic ordering temperature, which reduces in height and shifts to lower temperature on application of field. The shift of the peak confirms the antiferromagnetic nature of the compound. The inset shows the low temperature, zero field heat capacity data in an expanded scale, which shows two peaks; one near T_N and the other at 5 K. It may be

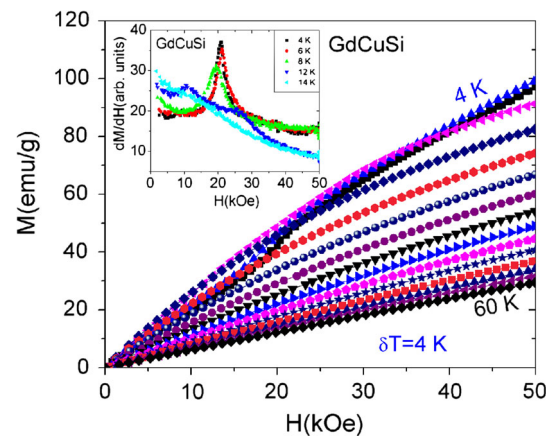


Fig. 4 Magnetization isotherms at selected temperatures for GdCuSi. *Inset* shows the derivative of magnetization plotted against field for GdCuSi

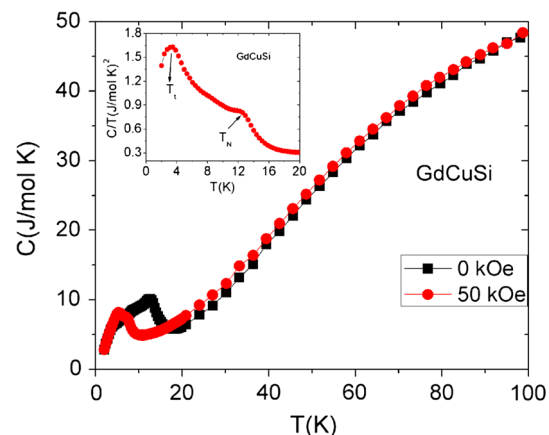


Fig. 5 Temperature dependence of heat capacity in zero and 50 kOe fields for GdCuSi. *Inset* shows the zero field data in an expanded scale

noted that these observations are in agreement with the magnetization data.

The magnetocaloric effect (MCE), in terms of isothermal magnetic entropy change (ΔS_M) and adiabatic temperature change (ΔT_{ad}), has been estimated using both magnetization (M-H-T) and heat capacity (C-H-T) data. The magnetization (M-H-T) data were used to calculate isothermal magnetic entropy change using the Maxwell's relation.

$$\Delta S_M = \int_0^H (\partial M / \partial T)_H dH. \quad (1)$$

ΔS_M and ΔT_{ad} were estimated from heat capacity (C-H-T) data using the relations

$$\Delta S_M(T, H) = \int_0^T \frac{C(T', H) - C(T', 0)}{T'} dT', \quad (2)$$

$$\Delta T_{ad}(T)_{\Delta H} = [T(S)_{H_f} - T(S)_{H_i}]_S. \quad (3)$$

The ΔS_M values estimated from M-H-T and C-H-T data at various fields are shown in Fig. 6. The compound shows negative ΔS_M (positive MCE) around its T_N and positive ΔS_M (negative MCE) near T_i . The maximum MCE for the field change of 50 kOe is found to be 8 J/kg K. Negative MCE may be due to the spin reorientation, as seen in the magnetization and the heat capacity data. One can note from Fig. 6 that the shapes of MCE estimated from M-H-T and C-H-T data are similar. The maximum value of ΔT_{ad} (inset of Fig. 6) is found to be 5.4 K for the field of 50 kOe, which is comparable to that of many compounds of RTX series working in the same temperature regime [1].

We have also performed the electrical resistivity measurement in presence of various fields and the data are shown in Fig. 7. The compound shows linear behavior and positive temperature coefficient of electrical resistivity in the paramagnetic regime, indicating the metallic character of the sample. Near T_N , the resistivity changes the slope and decreases sharply with decrease in temperature. It has

been observed that near T_N , the slope of resistivity is very sensitive to the field. The upper inset in Fig. 7 shows the temperature derivative of resistivity with the maximum corresponding to T_N and the minimum corresponding to T_i . Hence, it is clear that the nature of resistivity changes with temperature, below T_N .

The magnetoresistance (MR) versus T plot for GdCuSi is shown in Fig. 8. It is clear that the compound shows large negative MR near its T_N and changes its sign below T_N . The field dependence of MR at different temperatures is shown in the inset of Fig. 8. The magnitude of negative MR increases with decrease in temperature and attains a maximum at T_N . Below T_N , the MR is positive, which increases for lower fields and shows a decreasing tendency at higher fields. Above T_N , the moments are random, which align in the field direction on the application of a field, causing a decrease in resistivity (i.e., negative MR). Below T_N , the strength of the antiferromagnetic coupling becomes stronger on lowering the temperature. In this temperature regime, application of a field causes spin fluctuations, which result in an increase in the resistivity (i.e., positive

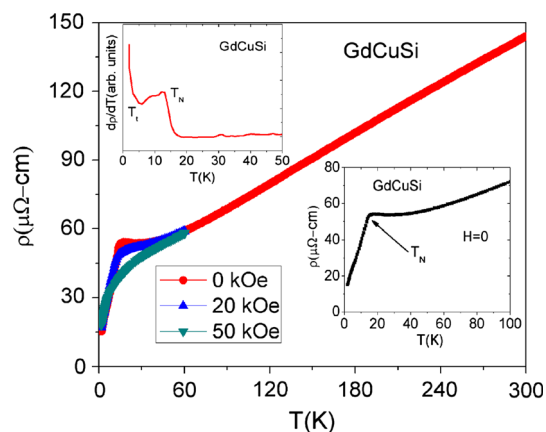
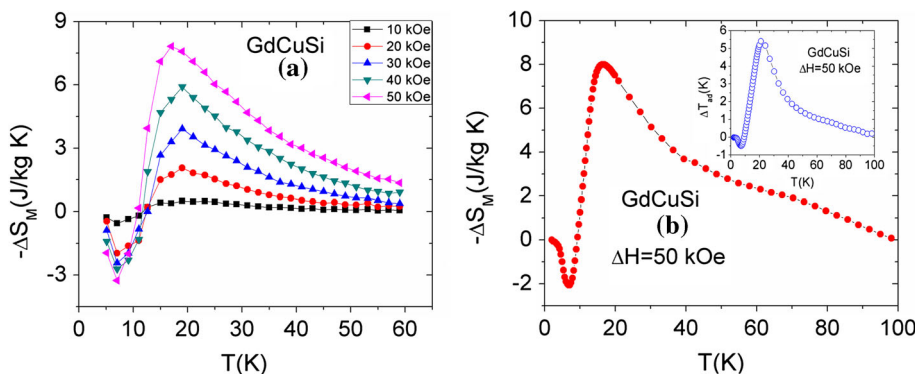


Fig. 7 Temperature dependence of electrical resistivity in 0, 20, and 50 kOe for GdCuSi. The upper inset shows the temperature derivative of electrical resistivity and the lower inset shows the zero field resistivity plot

Fig. 6 Temperature dependence of isothermal magnetic entropy change (a) calculated in various fields, calculated from M-H-T data (b) at 50 kOe, calculated from C-H-T data. The inset in (b) shows temperature dependence of ΔT_{ad} for field change of 50 kOe



MR). However, when the field is strong enough, the moments try to align in the field direction and results in a decrease in MR. The magnitude of MR near T_N and for a field of 50 kOe is found to be -27% . The MR shows a sign change below T_N with the maximum value of 22% for a field of 50 kOe. These values are larger than those observed in many RTX compounds [1].

Theoretical calculations

We have calculated the electronic structure and magnetic properties of GdCuSi using the LDA+U+SO method to account simultaneously for strong electronic correlations and to study the possibility of non-collinear magnetic ordering. The total and partial densities of states (DOS) of GdCuSi obtained in the self-consistent LDA+U+SO calculations are presented in Fig. 9, for simplicity one spin

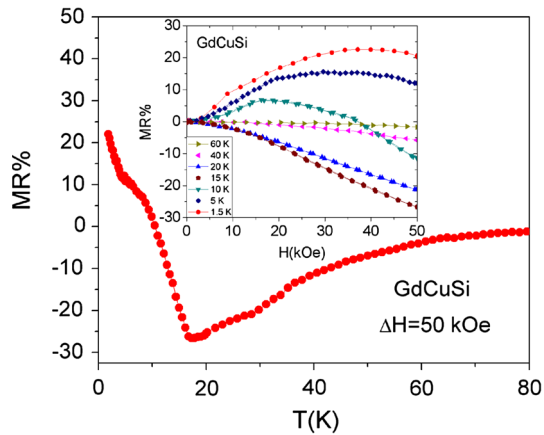


Fig. 8 Temperature dependence of MR in GdCuSi for a field of 50 kOe. The inset shows the field dependence of MR at different temperatures

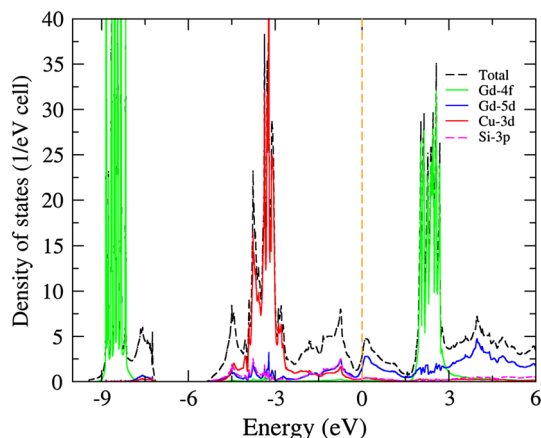


Fig. 9 Theoretical densities of states of GdCuSi obtained with the LDA+U+SO calculations. The Fermi level corresponds to zero

projection in the case of antiferromagnetic ordering is shown. At the Fermi energy (E_F), the total density of states of GdCuSi is mostly provided by the Gd 5d states, while the localized 4f states form a strong band centered at -8.5 eV below E_F for the states occupied with electrons and a band centered at 2.5 eV above E_F for the empty 4f states. The width of both bands is about 1 eV. In the case of ferromagnetic ordering of the Gd 4f states, these two bands are in the opposite spin projections. The other prominent part of DOS is the Cu 3d band found from -4 to -2.2 eV below E_F , these states of copper are almost fully occupied and are not spin-polarized. The other electronic states, like the Si 3p states shown in Fig. 9, have only minor contribution to the considered energy range near the Fermi energy.

From the LDA+U+SO calculations, strong magnetic moments of gadolinium ions with the effective magnetic moment of Gd $\mu_{\text{eff LDA+U+SO}} = 8.0 \mu_B$ were obtained, which is in very good agreement with the experimental value of $8.1 \mu_B$. As was already mentioned, the Cu ions are found non-spin-polarized with a negligible spin moment less than $0.1 \mu_B$. A non-collinear antiferromagnetic ordering of Gd moments was calculated as the ground state magnetic structure. The magnetic moment components are directed as $[-0.3, 0.2, 0.9]$ with the main contribution along z direction. Furthermore, a collinear antiferromagnetic solution is found to be slightly higher in total energy, while a non-collinear ferromagnetic ordering with the same direction of moments is also stable and is just 3 meV higher in total energy than the ground state. The closeness of the total energy ferromagnetic solution indicates the competing ferro and antiferromagnetic exchange interactions in the compound, which can promote spin reorientation at low temperatures, as observed in the experimental data.

Conclusions

In summary, we find that GdCuSi prepared in the present study possesses the Ni_2In -type hexagonal structure. It is clear from magnetic, heat capacity, magnetocaloric, and transport studies that GdCuSi shows antiferromagnetic ordering below 14.2 K and a spin reorientation at 5 K. A ferromagnetic component responsible for the non-collinear antiferromagnetic structure is inferred on the basis of experimental magnetization data as well as the theoretical calculations. The sign change seen in the temperature variations of MR and MCE is attributed to the non-collinear structure.

Acknowledgements SG thanks IIT Bombay for providing Research Associateship. The authors thank to UGC-DAE CSR, Indore and Dr.

R. Rawat for providing the facility of transport measurements. Theoretical calculations of the electronic structure were supported by the grant of the Russian Science Foundation (project No. 14-22-00004).

References

1. Gupta S, Suresh KG (2015) Review on magnetic and related properties of *RTX* compounds. *J Alloy Compd* 618:562–606
2. Bazela W, Szytuła A, Leciejewicz J (1985) Neutron-diffraction study of RECuSi (*RE* = Tb, Dy, Ho) intermetallic compounds. *Solid State Commun* 56:1043–1045 **and references therein**
3. Oesterreicher H (1976) Magnetic studies on compounds RCuSi, R₆Cu₈Si₈, and RCu₂Si₂ (R = Pr, Gd, Tb). *Phys Status Solidi (a)* 34:723–728
4. Mulder FM, Thiel RC, Buschow KHJ (1994) ¹⁵⁵Gd Mössbauer effect in AlB₂-type compounds. *J Alloy Compd* 205:169–174
5. Gignoux D, Schmitt D, Zerguine M (1986) Magnetic properties of CeCuSi. *Solid State Commun* 58:559–562
6. Oleś A, Duraj R, Kolenda M, Penc B, Szytuła A (2004) Magnetic properties of DyCuSi and HoCuSi studied by neutron diffraction and magnetic measurements. *J Alloy Compd* 363:63–67
7. Chen J, Shen BG, Dong QY, Sun JR (2010) Giant magnetic entropy change in antiferromagnetic DyCuSi compound. *Solid State Commun* 150:1429–1431
8. Chen J, Shen BG, Dong QY, Hu FX, Sun JR (2010) Giant reversible magnetocaloric effect in metamagnetic HoCuSi compound. *Appl Phys Lett* 96:152501-1–152501-3
9. Gupta S, Suresh KG, Nigam AK (2013) Interplay between magnetism and magnetocaloric effect in NdCuSi. [arXiv:1305.1124](https://arxiv.org/abs/1305.1124)
10. Schobinger-Papamantellos P, Ritter C, Buschow KHJ, Duong NP (2001) Magnetic phase diagram of ErCuSi studied by neutron diffraction and magnetic measurements. *J Magn Magn Mater* 223:203–214
11. Schobinger-Papamantellos P, Buschow KHJ, Ritter C (2004) Magnetic ordering of DyCuSi and HoCuSi studied by neutron diffraction. *J Alloy Compd* 384:12–21
12. Pöttgen R, Łątka K (2010) ¹⁵⁵Gd Mössbauer spectroscopy on intermetallics—an overview. *Z Anorg Allg Chem* 636:2244–2255
13. Iandelli A (1983) A low temperature crystal modification of the rare earth ternary compounds RCuSi. *J Less-Common Met* 90:121–126
14. Shorikov AO, Lukoyanov AV, Korotin MA, Anisimov VI (2005) Magnetic state and electronic structure of the δ and α phases of metallic Pu and its compounds. *Phys Rev B* 72:024458
15. Łątka K, Kmiec R, Pacyna AW, Fickenscher T, Hoffmann R-D, Pöttgen R (2004) Magnetism and ¹⁵⁵Gd Mössbauer spectroscopy of GdAuMg. *Solid State Sci* 6:301–309
16. Łątka K, Kmiec R, Pacyna AW, Fickenscher T, Hoffmann R-D, Rainer Pöttgen (2004) Magnetic Ordering in GdAuCd. *J Magn Magn Mat* 280(1):90–100
17. Hoffmann R-D, Fickenscher T, Pöttgen R, Felser C, Łątka K, Kmiec R (2002) Ferromagnetic ordering in GdPdCd. *Solid State Sci* 4:609–617
18. Gupta S, Suresh KG, Nigam AK, Mudryk Y, Paudyal D, Pecharsky VK, Gschneidner KA Jr (2014) The nature of the first order isostructural transition in GdRhSn. *J Alloy Compd* 613:280–287